molecular pharmaceutics

Article

pubs.acs.org/molecularpharmaceutics

Preparation and Characterization of Novel Magnetic Nano-in-Microparticles for Site-Specific Pulmonary Drug Delivery

Amber A. McBride,[†,‡,§] Dominique N. Price,[†,∥] Loreen R. Lamoureux,[†] Alaa A. Elmaoued,[†,‡] Jose M. Vargas,[⊥] Natalie L. Adolphi,[#] and Pavan Muttil*[,†,‡,§,∥]

[†]Department of Pharmaceutical Sciences, College of Pharmacy, [‡]Nanoscience and Microsystems Graduate Program, [∥]Biomedical Sciences Graduate Program, [§]The University of New Mexico Cancer Center, and [#]Department of Biochemistry and Molecular Biology, The University of New Mexico Health Sciences Center, Albuquerque, New Mexico 87131, United States

[⊥]The University of New Orleans, New Orleans, Louisiana 70148, United States

ABSTRACT: We propose the use of novel inhalable nano-in-microparticles (NIMs) for site-specific pulmonary drug delivery. Conventional lung cancer therapy has failed to achieve therapeutic drug concentrations at tumor sites without causing adverse effects in healthy tissue. To increase targeted drug delivery near lung tumors, we have prepared and characterized a magnetically responsive dry powder vehicle containing doxorubicin. A suspension of lactose, doxorubicin and Fe_3O_4 superparamagnetic iron oxide nanoparticles (SPIONs) were spray dried. NIMs were characterized for their size and morphological properties by various techniques: dynamic light scattering (DLS) and laser diffraction (LS) to determine hydrodynamic size of the SPIONs and the NIMs, respectively; next generation cascade impactor (NGI) to determine the aerodynamic diameter and fine particle fraction (FPF); scanning (SEM) and transmission (TEM) electron microscopy to analyze particle surface morphology; electron dispersive X-ray spectroscopy (EDS) to determine iron loading in NIMs; inductively coupled plasma atomic emission spectroscopy (ICP-AES) and superconducting quantum interference device (SQUID) to determine Fe_3O_4 content in the microparticles; and high performance liquid chromatography (HPLC) to determine doxorubicin loading in the vehicle. NIMs deposition and retention near a magnetic field was performed using a proof-of-concept cylindrical tube to mimic the conducting airway deposition. The hydrodynamic size and zeta potential of SPIONs were 56 nm and −49 mV, respectively. The hydrodynamic and aerodynamic NIM diameters were 1.6 μm and 3.27 ± 1.69 μm, respectively. SEM micrographs reveal spherical particles with rough surface morphology. TEM and focused ion beam−SEM micrographs corroborate the porous nature of NIMs, and surface localization of SPIONs. An *in vitro* tracheal mimic study demonstrates more than twice the spatial deposition and retention of NIMs, compared to a liquid suspension, in regions under the influence of a strong magnetic gradient. We report the novel formulation of an inhaled and magnetically responsive NIM drug delivery vehicle. This vehicle is capable of being loaded with one or more chemotherapeutic agents, with future translational ability to be targeted to lung tumors using an external magnetic field.

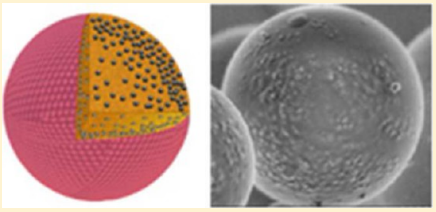

KEYWORDS: *pulmonary delivery, magnetic microparticles, inhalable dry powders, SPIONs, lung cancer therapy, spray drying*

1. INTRODUCTION

Lung cancer is the leading cause of cancer mortality worldwide, with 1.4 million people dying from the disease each year, as of 2008.[1] Lung cancer accounts for more deaths than breast, prostate, colon, liver and kidney cancers combined.[2] In the United States alone, 160,000 people died of lung cancer in 2010.[3] Despite the use of new chemotherapeutic agents for lung cancer, the average patient five-year survival rate is 5−15% and has remained largely unchanged for decades.[1]

These statistics are due, in part, to conventional drug delivery systems that neither deliver nor maintain sufficient drug concentration near solid lung tumors,[4] leading to adverse effects in healthy tissues. The lung offers a unique and challenging route for drug delivery with high absorption and surface area, ca. 100 m^2.[2,5] Inhaled drug delivery is widely used for diseases such as asthma, COPD and cystic fibrosis and has shown promise as an alternate delivery method for lung cancer chemotherapeutics. However, it has been associated with side effects.[6]

A major unmet medical need in the field of cancer therapy is to selectively deliver chemotherapeutic agents to lung tumors. The objective is to minimize side effects observed in healthy lung tissues as well as to achieve effective therapy. A phase I/II study of inhaled doxorubicin combined with oral cisplatin and docetaxel-based therapy for advanced non-small cell lung cancer showed the efficacy of inhaled therapy. Although seven evaluable patients responded to the combined inhaled and oral therapy, dose-limiting pulmonary toxicity was observed in two patients due to a lack of drug-tumor targeting.[7,8] This

Received: December 22, 2012
Revised: August 19, 2013
Accepted: August 21, 2013
Published: August 21, 2013

study showed the benefit of delivering agents directly to the lung with diminished systemic side effects.

Researchers have used Fe_3O_4 superparamagnetic iron oxide nanoparticles (SPIONs) as a means to target drugs to specific regions of the lung in animal models to mitigate the toxicity observed in healthy lung tissues.[9−11] If successful, this approach will lead to improved tumor targeting, minimize the side effects observed in healthy tissues due to the chemotherapeutic agent, and maximize the therapeutic outcome. Targeted pulmonary drug delivery using SPIONs will also significantly lower the total drug dose required to achieve therapeutic response at the tumor site, thus further alleviating the side effects observed in healthy tissues.

Previously, Dames, et al.[11] and Rudolph et al.[12] targeted nebulized suspension containing SPIONs and pDNA, a therapeutic mimic, to specific regions in a mouse lung. Although significant deposition of SPIONs was shown in the magnetized lobe, separation of pDNA from SPIONs during the delivery process was observed. Nebulized formulations used in these studies lead to separation of the drug surrogate from the SPIONs before reaching the intended target site. We propose formulating and characterizing an inhalable dry powder vehicle containing SPIONs and a chemotherapeutic agent. This novel approach overcomes the natural deposition mechanism of inhaled aerosol liquid droplets in the lungs that is limited by targeting of aerosols to the central and peripheral airways but not to local regions of the lung.

The objective of this study was to formulate and characterize nano-in-microparticles (NIMs) containing SPIONs and the chemotherapeutic agent doxorubicin in a lactose matrix. NIMs, the first of their kind formulated in a dry powder form, will prevent premature separation of the chemotherapeutic agent and SPIONs.[13]

2. EXPERIMENTAL SECTION

2.1. Materials. Alpha-D-(+)-lactose monohydrate Respitose ML-001 was a gracious gift from DMV-Fonterra Excipients GmbH & Co. KG (Goch, Germany). FluidMAG-UC SPIONs with a hydrodynamic diameter of 50 nm were gifted and purchased from Chemicell GmbH (Berlin, Germany). Fluoro-Max Green Fluorescent Polymer nanospheres (0.025 μm diameter) were purchased from Thermo Fisher Scientific. Adriamycin (doxorubicin) was purchased from Selleck Chemicals, LLC (Houston, TX). A Gemini-NX 5 μm C18 110 A 150 × 4.6 mm HPLC column was purchased from Phenomenex (Torrance, CA). OmniSolv acetonitrile, anhydrous, was obtained from EMD Chemicals (Gibbstown, NJ), and all other reagents were of analytical grade and used as received. Borosilicate glass tubes (20 mm × 120 mm) were fabricated by Scientific Glass Co. Ltd. (Albuquerque, NM). A commercially available neodymium−iron−boron (NdFeB) permanent cylindrical magnet (grade N52, 22 mm long × 20 mm in diameter) was purchased from Applied Magnets (Plano, TX).

2.2. Preparation of Inhalable Magnetic Microparticles. NIMs containing fluorescent nanospheres or a chemotherapeutic agent (doxorubicin) were prepared by spray drying. A suspension containing 78.2% lactose, 20% SPIONs and 2.8% doxorubicin (w/w) in double distilled water (ddH_2O) was spray dried using a mini-spray dryer B-290 with a standard two-fluid nozzle (0.7 mm diameter) (Büchi Corporation, Flawil, Switzerland). NIMs were also formulated with a fluorescent nanosphere drug-surrogate; the drug was replaced with 4.0% nanospheres (w/w). Nanospheres were used in the NIM formulation, rather than a soluble dye, to avoid redistribution of free dye following deposition in unmagnetized regions. Spray drying parameters were the same for nanospheres and doxorubicin-containing NIMs and were as follows: inlet temperature 170 ± 2 °C, outlet temperature 103 ± 2 °C, aspirator rate 100%, pump flow rate of 10% and air flow rate 742 L/h. Control lactose particles were prepared by spraying a 5% lactose solution (w/v) in ddH_2O using the above parameters. When spray drying doxorubicin and SPIONs, the spray dryer was isolated in a walk-in chemical hood that was vented to outside air to prevent exposure to toxic vapors. Chemotherapeutic-resistant PPE was worn when handling doxorubicin and NIMs.

2.3. Microparticle Characterization. *2.3.1. Yield and Encapsulation Efficiency of Doxorubicin.* NIM yield was calculated as the ratio of the mass of solids collected after spray drying to the amount of solids in the feed suspension. The percentage encapsulation efficiency (EE) and percentage doxorubicin loading in NIMs were determined using eqs 1 and 2, respectively:

$$\%\ \mathrm{EE} = \frac{\text{actual weight of doxorubicin in NIMs} \times 100}{\text{theoretical weight of doxorubicin in NIMs}} \quad (1)$$

$$\%\ \text{doxorubicin loading} = \frac{\text{actual weight of doxorubicin in NIMs} \times 100}{\text{NIMs weight}} \quad (2)$$

2.3.2. SPION Characterization: Hydrodynamic Size and Zeta Potential. Hydrodynamic size (D_{50}) was determined using dynamic light scattering (Zetasizer Nano ZSP, Malvern Instruments Ltd.). The samples were prepared by dispersing 1 μL [50 mg/mL] of SPIONs in 1 mL of ddH_2O (n = 9). The zeta potential of SPIONs was characterized by dispersing 0.5 μL [50 mg/mL] of SPIONs in 1 mL of ddH_2O (n = 9), expressed as size distribution by average intensity.

2.3.3. NIM Hydrodynamic Size. The volume median diameter (D_v 0.5) of the NIMs was determined by laser diffraction using the cuvette disperser (Helos/KF-OM, Sympatec GmbH, Germany). Briefly, 5.0 mg of NIMs was suspended in 1 mL of acetonitrile and gently vortex-mixed. A 200 μL aliquot of this suspension was added dropwise to the 6 mL cuvette containing 5 mL of acetonitrile. Measurements were taken for 10 s using the R3 lens in triplicate.

2.3.4. In Vitro Aerosolization Studies (Aerodynamic Diameter). The aerodynamic size of the spray dried NIMs containing dye was determined using a Next Generation Impactor (model 170 NGI, MSP Corporation, Shoreview, MN). NIM samples (6 mg) were aerosolized using a model DP4 dry powder insufflator for rat (Penn Century, Inc., USA). A pump (Copley Scientific, Nottingham, U.K.) was operated at a flow rate of 30.0 L/min for 10 min. Following aerosolization, particle deposition was measured by gravimetric method from collection cups. The percent cumulative mass fractions were plotted versus log aerodynamic diameters. The mass median aerodynamic diameter (MMAD) was estimated by linear interpolation that links the curve points at 50% deposition. The fine particle fraction (FPF; stage 3 to stage 7, i.e. <6.4 μm) was calculated as a percentage of total emitted dose (n = 3).

2.3.5. NIM Morphology and Cross Sectional Analysis. To determine particle size, surface morphology and elemental analysis, NIMs were visualized using a high-resolution scanning

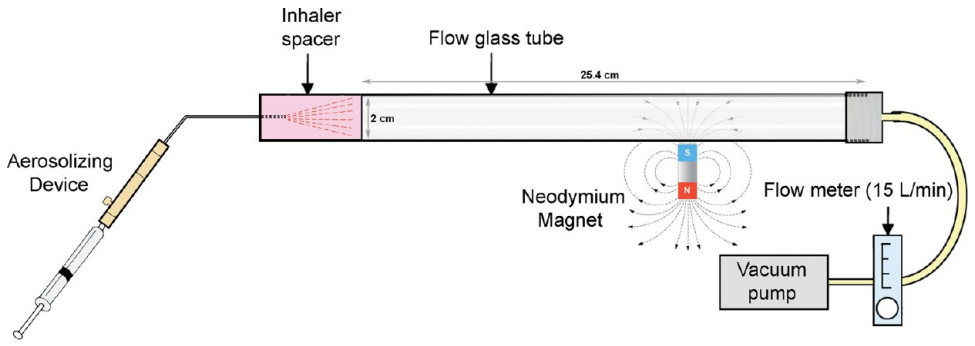

Figure 1. Tracheal mimic tube study. A tracheal mimic tube was fitted with an inhaler spacer and connected to vacuum pump mimicking breathing inspiration, determined by a flow meter at 15 L/min. A neodymium magnet was placed in a region of interest, and formulations of either NIMs or liquid suspension were administered.

electron microscope energy dispersive X-ray spectrometry (EDS-SEM) (JEOL 5800LV). Briefly, NIMs were deposited onto a small piece of silicon wafer using double-sided magnetic adhesive tape and examined in the SEM at 0.3−20 kV. Using the focused ion beam SEM (FIB-SEM), electron-transparent slices of the NIMs were cut to reveal a cross-section of the microparticle. For transmission electron microscopy (TEM, JEOL 200CX TEM operated at 200 kV), NIMs were uniformly suspended in acetonitrile and 10 μL droplets were mounted on copper grids covered with holey carbon film. Samples were also analyzed by energy dispersive X-ray spectroscopy (EDS) for SPION loading in NIMs.

2.3.6. Iron Content Determination. To evaluate concentrations of Fe in NIMs, samples were analyzed using inductively coupled plasma atomic emission spectroscopy (ICP-AES, Perkin-Elmer Elan II, Waltham, MA). The internal standard was iron (Fe) at mass 55.845. The analysis was performed comparably to method US EPA 200.8. Exactly 10 mL of the standards, samples, and QC samples were spiked with 1 mL of 100 mg/L Fe as internal standard to correct for drifts in the signal that may be caused by sample matrix, viscosity of the solution, and/or peristaltic pump (sample) pulsing. The system was calibrated using NIST traceable calibration standards (stock solution) and QC solutions (stock solution). The system is sensitive down to the parts per billion (ppb) level. Three milligram NIM samples were taken for measurement and digested, using 2 mL of nitric acid, at 90 °C. After digestion was completed, digests were brought up to 10 mL final volume and transferred into ICP plastic tubes. Results were then calculated using the starting weight and the final volume after digestion. Results were expressed as μg/g of Fe and then converted to ppb based on the standard curve. Fe was calculated based on the basis of the molecular ratio of Fe_3O_4. Samples were run in duplicate.

2.3.7. Doxorubicin Content Determination Using HPLC. We adapted an HPLC method reported by Mikan et al.[14] and Urva et al.[15] A stock standard of 65 μg/mL was prepared by placing 0.65 mg of doxorubicin into a 10 mL volumetric flask and diluted in pH 3.0 ddH_2O to a total volume of 10 mL. A working standard of 20 μg/mL was prepared by transferring appropriate amounts of stock doxorubicin in a 5 mL volumetric flask and diluted in pH 3.0 water to a total volume of 5 mL. Both stock and working doxorubicin solutions were stored at 4 °C. To create a standard curve, doxorubicin standards with concentrations of 0.078, 0.156, 0.31, 0.63, 1.25, 2.5, 5, 10, and 20 μg/mL were prepared by accurately transferring appropriate volumes of working doxorubicin solution to HPLC vials. NIM concentrations of 2 and 14 μg/mL were prepared by dispersing NIMs into a suspension, separating the SPION component using a magnetic gradient, and transferring supernatant to HPLC vials. The HPLC system consisted of a 1260 Infinity Agilent LC (Agilent Technologies, Santa Clara, CA). Integrations, calculations, and plotting of chromatograms were performed with a Chemstation computing integrator (Agilent Technologies, Houston, TX). A C18 HPLC column was used, and the mobile phase was prepared by mixing acetonitrile and water, adjusted to pH 3.0 with phosphoric acid, at 72/28 (v/v) proportions. Doxorubicin eluted at 7.2 min with a flow rate of 1 mL/min. The UV detector was set at a wavelength of 254 nm. The HPLC apparatus was operated at room temperature.

2.3.8. SPION Magnetization Measurement. Magnetic properties were measured with an MPMS-7XL SQUID Susceptometer (Quantum Design, San Diego, CA) integrated to a Physical Properties Measurement system (PPMS, Quantum Design, San Diego, CA). The ac susceptibility measurements were conducted in the temperature range from 4 to 300 K with nominal magnetic field of 20 kOe. These measurements allowed us to calculate the magnetic moment of the SPIONs as well as the concentration of SPIONs in the NIMs.

2.3.9. Permanent Magnet Characterization. The cylindrical permanent magnet (2.5 cm length × 2 cm diameter) was characterized using a Bell-5180 series Hall effect gauss/teslameter and an STD18-0404 axial gaussmeter probe (Sypris Test and Measurement, F.W. Bell, Orlando, FL). The Hall effect gaussmeter was used to measure the flux density (B) at increasing distances from the surface of the magnet. A ruler was taped parallel to the magnet, and the flux density was measured with the axial gaussmeter probe in 1 mm increments from a distance of zero to 30 mm from the magnet. Because magnetic force is proportional to the magnetic field gradient ($\Delta B/\Delta x$, in units of G/mm), the gradient was determined by dividing ΔB, the change in the flux density between each successive measurement, by Δx, the change in distance between each successive measurement. The magnetic field gradient measurements were used to indicate the relative strength of the magnetic attractive force on the NIMs at different positions for the subsequent tracheal mimic tube study.

2.4. Proof of Concept Tracheal Mimic Tube Study. Cylindrical borosilicate glass tubes were designed and fabricated to mimic the conducting airways of the human respiratory tract. The dimensions of the tube were similar to those of a human male adult (20 mm diameter × 200 mm length × 1 mm

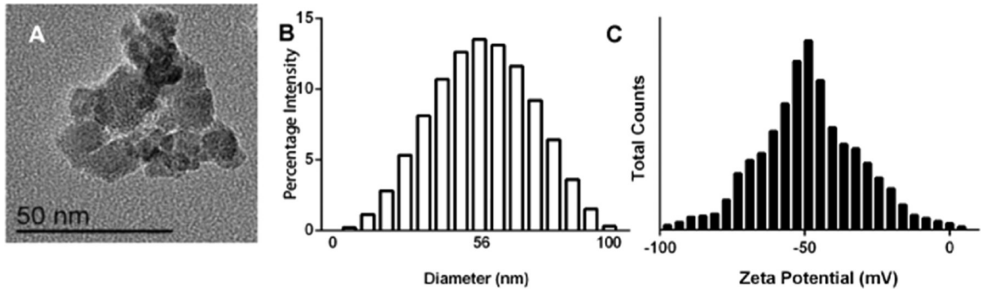

Figure 2. Hydrodynamic size and stability characterization of SPIONs. SPIONs are a component of the NIM drug delivery vehicle. (A) The transmission electron microscopy (TEM) micrograph shows monodisperse 50 nm diameter single-domain Fe_3O_4 nanoparticles. (B) Dynamic light scattering (DLS) shows a D_{50} of 56 nm. (C) Zeta-potential shows nanoparticle charge of −49 mV.

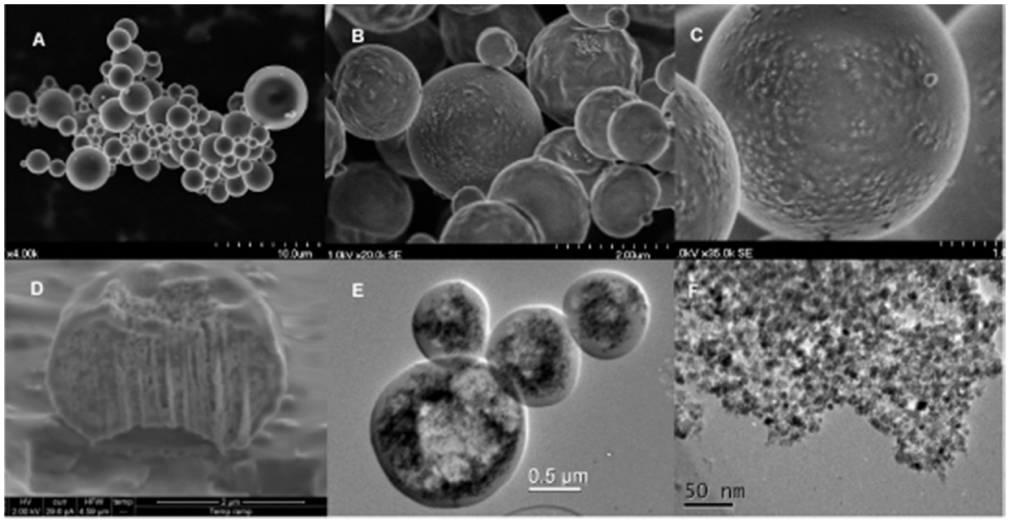

Figure 3. SEM images of (A) lactose particles. (B, C) NIMs containing SPIONs, doxorubicin and lactose. (D) A cross-section of a single NIM ablated with a focused ion beam. (E) TEM images of electron-dense SPIONs concentrated toward the outer surface of NIMs. (F) A magnified version of E showing the distribution of SPIONs.

thickness). Two different formulations were examined: NIMs and a nebulized liquid suspension. Both formulations contained the green fluorescent nanospheres as a surrogate for doxorubicin. Briefly, 5.0 mg of NIMs was weighed for each run; for the preparation of the liquid suspension 5.0 mg of the NIMs were suspended in 3 mL of water to have equal proportions of the nanospheres and SPIONs. The permanent magnet was placed on the external vertical axis of the tube to achieve retention of the NIMs near the magnet (Figure 1).

The magnetic retention of the NIMs was examined by placing the magnet at 0 and 4 mm from the tube based on the magnetic strength characterized earlier. These two distances were measured from the outer surface of the glass tube (thickness 1 mm). Aerosol generators (model DP-4 dry powder insufflator and model IA-1C liquid suspension microsprayer (Penn Century, Inc., Philadelphia, PA, USA)) were used to aerosolize the NIMs and the liquid suspension, respectively (n = 3) (Figure 1). The glass tube was connected to a vacuum source that was adjusted to a flow rate of 15 L/min. Relative fluorescence intensity was quantified using the Carestream Molecular Image Station 4000 MM Pro using excitation and emission wavelengths of 488 and 508 nm, respectively. Student t tests were used to quantify statistical significance (Graphpad prism, La Jolla, CA).

3. RESULTS

3.1. NIM Formulation. NIMs were formulated by spray drying doxorubicin and SPIONs in a lactose matrix. For the purpose of drug delivery and bioavailability to tumors, NIMs were characterized on the basis of size, surface morphology and magnetic properties. SEM and TEM micrographs indicate NIMs to be spherical in shape with a diameter of 1.6 μm (Figure 3C and Figure 3E, respectively). TEM micrographs revealed increased electron dense (black) areas indicating the presence of iron atoms. Cross-sectional analysis by TEM shows that SPIONs are preferentially distributed on the outer surface of the NIMs (Figure 3E). SEM micrographs revealed a rough outer surface due to SPIONs protruding from the lactose matrix (Figure 3C). The surface area of NIMs may be influenced by the extent of the surface roughness. This is an important characteristic of dry powers when mitigating drug−drug particle agglomeration formation.[16]

3.2. Characterization of SPIONs: Hydrodynamic Size, Zeta Potential, and TEM. SPIONs had an average radius of 56 ± 6 nm (Figure 2B) and a density of 2.5 g/cm^3. SPIONs had an average zeta potential of −49 mV (Figure 2C) and confer colloidal stability against aggregation. TEM micrographs of SPIONs showed magnetite crystals on the order of 6 nm that are combined to form a single-domain 50 nm core (Figure 2A).

3.3. Yield, Encapsulation Efficiency and Doxorubicin Loading. The theoretical powder yield was 60.9% based on a

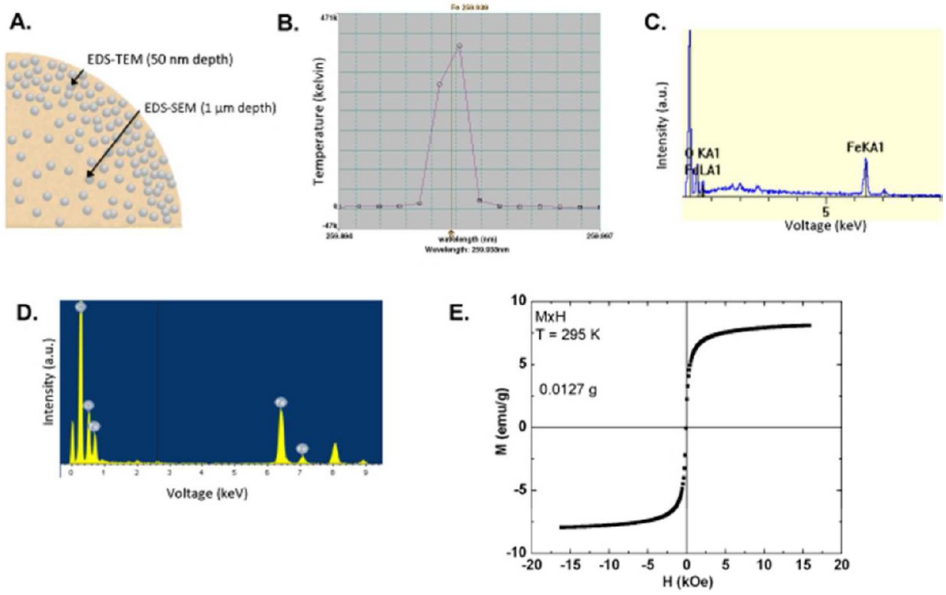

Figure 4. Quantification of Fe_3O_4 in NIMs. (A) Schematic depicting cross-section NIMs and SPION localization. (B) ICP-AES chromatogram of Fe_3O_4 loading in NIMs. (C) EDS/SEM Fe depth analysis. (D) EDS/TEM Fe depth analysis. (E) Hysteresis curve shows superparamagnetism and demonstrates the total electromagnetic unit (emu), enabling the calculation of Fe_3O_4.

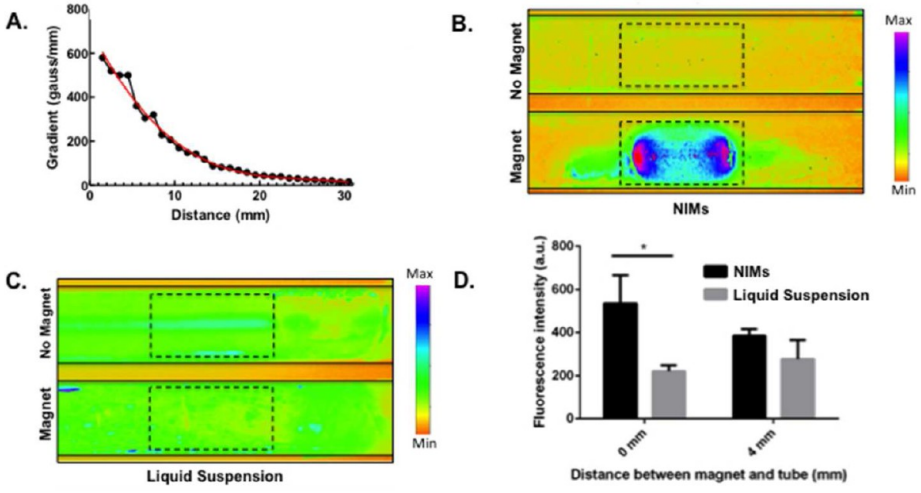

Figure 5. A cylindrical glass tube was designed to mimic the conducting airway of the human pulmonary tract. (A) Magnetic gradient characterization of a permanent magnet used to direct and retain NIMs to a region of interest. The magnet was characterized over a distance of 30 mm and fit with the function $1/x^3$. (B) The targeting and retention of a fluorescent dye with and without a magnet using NIMs. (C) The targeting and retention of a fluorescent dye with and without a magnet using a liquid suspension. The magnetic retention of the NIMs was examined by placing the magnet at 0 and 4 mm from the tube. These two distances were measured from the outer surface of the glass tube (thickness 1 mm). (D) The NIMs formulation is 2.4 times more fluorescent in a magnet region of interest (p = 0.0154).

mass balance performed on the solids (SPIONs, doxorubicin, lactose) and NIMs before and after spray drying, respectively. Using HPLC, % EE was quantified in NIMs to be 57%. Doxorubicin eluted with a retention time of 7.2 min. Theoretically, NIMs contained 2.8% (w/w solids) doxorubicin, and actual doxorubicin loading was quantified to be 1.6%. The doxorubicin loss is attributed to the spray drying process; small particles of doxorubicin (which have a characteristic red color) were visually observed trapped in the filter of the machine.

3.4. NIM Characterization. The average hydrodynamic NIM diameter was 1.6 μm using laser diffraction. This size correlates with the size assessed using SEM (Figure 3B). A MMAD of 3.27 μm was obtained using a NGI. The aerodynamic diameter takes the density of the NIMs into account and is fundamental to particle deposition in the lung and hence for inhaled drug delivery. The average fine particle fraction (FPF) ($\leq$6.4 μm) of the NIMs was >90%, and the geometric standard deviation (GSD) was $\pm$1.69.

3.5. Permanent Magnet Characterization. Single and two combined permanent magnets were characterized for their magnetic field strength. The magnetic field strength on the surface of the single magnet was 0.58 T. Magnetic field strength did not increase when two permanent magnets were combined (data not shown). Magnetic field lines are parallel to the surface of the magnet and diverge with increasing distance, resulting in a weaker flux density at larger distances; the magnetic force acts on the NIMs when they enter this region of diverging magnetic field. The direction of the force moves magnetic objects from

dx.doi.org/10.1021/mp3007264 | Mol. Pharmaceutics 2013, 10, 3574−3581

regions of lower flux density to regions of greatest flux density (i.e., the surface of the magnet). This study also shows that the geometry and orientation of the magnet is critical for significant deposition of the NIMs near the magnet.[9] Figure 5A shows that the magnet was characterized over a distance of 30 mm with decreasing magnetic gradient strength (G/mm).

3.6. Magnetization Measurement. A SQUID is a sensitive magnetometer that is used to measure extremely small magnetic fields, and with this device we measured the magnetic moment of NIMs. Susceptibility curves were obtained to provide the specific magnetization (s) in emu/g at a particular magnetic field strength. This is related to the susceptibility through the equation $\chi = (s^*\rho)/H$ where ρ is the particle density. The zero coercivity and the reversible hysteresis behavior indicate the superparamagnetic nature of the SPIONs (Figure 4E). The specific saturation magnetization for the NIM formulation was 8 emu/g. This value is below the saturation magnetization known for bulk Fe_3O_4 (M_s = 92 emu/g) as expected given that lactose does not contribute to the magnetic moment. The magnetization measurement suggests that the NIMs are approximately 9% Fe_3O_4 by weight. The magnetization was corrected by the diamagnetic response of the sample-holder, and normalized by sample mass.

Using ICP-AES, elemental Fe in NIMs was 7.67%. When converting this to magnetite, Fe_3O_4 was calculated to be 10.6% by weight, in good agreement with the Fe_3O_4 fraction obtained from the magnetization measurements (9%). EDS-SEM and EDS-TEM quantified Fe on the NIM surface, and Fe_3O_4 was calculated to be 16 ± 0.5% and 19 ± 0.5%, respectively (Figure 4C,D). These numbers are further understood knowing that EDS-TEM has a depth resolution of 50 nm whereas EDS-SEM penetrates an average sample depth of ~1 μm.[17] TEM micrographs (Figure 3E) qualitatively supported this observation that SPIONs are less densely distributed/localized in the center of the NIMs. Thus EDS-SEM quantitates a lower amount of Fe_3O_4 given this analytical tool penetrates the sample more deeply than EDS-TEM.

3.7. Proof of Concept Tracheal Tube Study. Magnetic retention of NIMs containing fluorescent nanospheres was quantified in relation to its fluorescence intensity (Figure 5B,C). Quantitative fluorescence analysis showed a 2-fold increased deposition of aerosolized NIMs at 0 mm (mean = 534.97, SD = 131.17) near the magnet based on greater fluorescence intensity, compared to the aerosolized liquid formulation at 0 mm (mean = 221.67, SD = 26.70) (t = 4.054, p = 0.0154, df = 4, two-tailed Student t test) (Figure 5B,C,D). Control studies of untargeted NIMs (absence of magnetic targeting) qualitatively show no mean fluorescence over background in the region of interest (Figure 5B,C). Quantitative fluorescence analysis showed increased deposition of NIMs at 4 mm (mean = 385.65, SD 30.15), compared to the aerosolized liquid formulation (mean 277.30, SD = 88.16) (Figure 5D). A 28% decrease in the fluorescence intensity of NIMs was observed when the magnet was placed 4 mm away from the tube compared to 0 mm.

4. DISCUSSION

This research proposes the use of regional chemotherapy by the pulmonary route with the intent of increasing drug exposure near a solid tumor. Despite inhaled drug delivery being used for respiratory diseases for over 30 years,[18] targeted drug delivery to specific regions of the lung has not been adequately explored. We show here, for the first time, the formulation of magnetic NIMs containing SPIONs and doxorubicin, by the process of spray drying. NIMs can be guided to a region of interest in a tracheal tube with strategic placement of an external magnet. Inhalable dry powders will allow higher doses of drug to be delivered to cancerous lung regions without increasing side effects observed in surrounding healthy tissues, compared to a liquid suspension. Using this novel delivery method, we do not expect to overcome oropharyngeal deposition. This delivery method will only localize drug near the target region that does not impact the upper regions of the respiratory tract.

4.1. Formulation of a Novel Inhalable NIMs Delivery Vehicle. NIMs were formulated using pulmonary-compatible lactose rather than a biodegradable polymer. This is to allow for the immediate release of drug from the vehicle after deposition and to minimize the patient contact time with the magnetic field. After NIM deposition at the target site, the NIM will disintegrate quickly in the lung parenchyma to release drug that will diffuse into the target tumor mass. Neither doxorubicin nor SPIONs are conjugated to the delivery vehicle thus eliminating any limitations on the release of bound drug near the target site.

4.2. Characterization of NIMs. NIMs exhibit a rough outer surface, as seen from the SEM images (Figure 3B,C). This facilitates a beneficial disaggregation of particles when administered as a dry powder.[16] Currently, dry powder flow and dispersion are improved by incorporating larger particles (50−100 μm) as carriers[19] to facilitate disaggregation of dry powders during inhalation. Should NIM flow or dispersion be a problem, the addition of carrier particles would be considered. The flow dynamics of the NIMs after inhalation can also affect the drug deposition and would require further studies. A logical next step, and our next pursuit, will involve the administration of NIMs in animal models to investigate the targeting capabilities in the upper and lower respiratory tract.

NIMs can be designed to modulate drug release after the particles have been guided to the targeted lung regions in the future. If this concept is successful, NIMs can also be used to deliver doublet chemotherapeutic agents since doublet therapy is the cornerstone of treatment for lung cancer. Future studies also need to investigate the effect of SPIONs on cellular uptake and pulmonary toxicity in animal models, since surface properties of SPIONs are known to affect the cellular uptake and cytotoxicity. However, the biodegradability and biocompatibility of SPIONs have been proven for many years in the clinical setting as a contrast agent in magnetic resonance imaging.[20,21]

4.3. Magnetic Properties of Aerosolized NIMs. The small magnetic moment of individual SPION in an aerosolized liquid droplet cannot be guided easily in the presence of an external magnet. However, when SPIONs are assembled together in NIMs,[16] the net magnetic moment of aggregated SPIONs is large enough to be manipulated with a medically compatible external magnet. In addition, droplets containing nanosized SPIONs for inhaled drug delivery are easily exhaled due to their small size; therefore encapsulating the SPIONs into micrometer sized NIMs will help to resolve this problem. The combined magnetic moment of the SPIONs present in the NIMs may allow the particles to be retained at the target site until the NIMs disintegrate therefore releasing the drug. In addition, NIMs could also be retained at the target site by entrapment from lung mucus and cilia.

A 28% decrease in the fluorescence intensity of NIMs was observed when the magnet was placed 4 mm away from the

tube compared to 0 mm. This decrease in fluorescence, and therefore magnetic force, is a challenge that needs to be addressed since the magnetic field has to penetrate a larger distance if this targeting mechanism is to be applied in humans. Since the magnetic gradient decreases with the distance to the target tissue, the main limitation of this delivery mechanism could relate to the strength of the external field that can be applied to the patient to obtain the necessary magnetic gradient; however, high field gradient electromagnets are being used in animals for magnetic targeting[22] and substantial field gradients are also used in MRI imaging. Further studies are needed to validate the safety of the strength of an external magnet as it relates to magnetic nanoparticles.

The magnetization s-curve of NIMs loaded with 9% w/w Fe_3O_4 is shown (Figure 4E) and has negligible coercivity, and consequently no remanence was observed once the magnetic field was removed, indicating the superparamagnetic behavior of the SPIONs. Localization of SPIONs on the NIM surface was qualitatively and quantitatively observed. Surface analytical techniques were used to understand the elemental depth profiles of SPIONs in NIMs. EDS analysis is based on the beam voltage which is applied to the sample; a lower voltage will excite electrons to a lesser depth in the sample allowing for the quantification of elemental Fe composition. Both EDS-TEM and EDS-SEM analysis were used to determine the distribution of SPIONs in the NIMs from the surface to the interior of the particles (Figure 4C,D). Uncoated SPIONs were chosen for this formulation to exploit the superparamagnetic properties of the core iron oxide nanoparticles, since coating leads to loss of magnetic strength[23] per volume. However, coating SPIONs with a polymer is known to prevent aggregation and to provide colloidal stability to the suspension. In our study, the suspension containing SPIONs, drug and lactose was adequately stirred prior to and during the spray drying process, to prevent aggregation of SPIONs.

4.4. Proof-of-Concept Tracheal Mimic and NIMs Targeting. Dames et al.[11] and Hasenpusch et al.[24] have proven the feasibility of magnetic aerosol delivery using nebulized SPIONs and a drug surrogate to target specific lung regions in mice using an external permanent magnet. A drawback of this delivery system was that the drug surrogate separated from the magnetic carrier during pulmonary delivery resulting in premature release of the surrogate in the upper respiratory tract. This separation would result in a lower amount of the drug surrogate reaching the target site in a liquid suspension. We demonstrated a similar result in the tracheal mimic experiment as seen by a uniform nanosphere distribution in the tube of a liquid suspension formulation (Figure 5C). In contrast, the NIM formulation showed significant spatial deposition of dye only in regions experiencing a strong magnetic force (Figure 5B). The targeting of NIMs resulted in a fluorescent intensity that was 2.4 times more than that of the liquid formulation near the magnet at 0 mm distance (Figure 5D). It is to be noted that the tracheal mimic experiment exhibits the *in vitro* targeting and retention of dry powders for a proof of concept idea, and the aerosol particles were assumed to be carried by a laminar airstream, consistent with other published literature.[9,10] However, we do expect turbulence to be generated when NIMs are near the magnetic field. Guiding NIMs containing SPIONs to a specific lung lobe will be challenging because it is more complex than the single tube we have used in this study.

This study brings about new perspectives for specific disease treatment by increasing delivery of chemotherapeutic agents to the tumor mass and reducing unwanted drug-related side effects in nondiseased tissue. In conclusion, SPIONs with very high saturation magnetization were successfully encapsulated in NIMs by spray drying. These novel formulations have the potential to be targeted to specific regions of the lung using an external magnet.

AUTHOR INFORMATION

Corresponding Author

*College of Pharmacy, Department of Pharmaceutical Sciences, 2705 Frontier NE, Suite 208-7, Albuquerque, New Mexico 87131, United States. E-mail: pmuttil@salud.unm.edu.

Notes

The authors declare no competing financial interest.

ACKNOWLEDGMENTS

We thank Dr. Mehdi Ali for his assistance analyzing Fe quantification, and Ms. Erin Weeda for her help with the tracheal mimic tube studies. We also thank the New Mexico Cancer Nanotechnology Training Center and fellowship program for their support.

ABBREVIATIONS USED

MMAD, mass median aerodynamic diameter; NIMs, nano-in-microparticles; SPIONs, superparamagnetic iron oxide nanoparticles; ICP-AES, inductively coupled plasma atomic emission spectroscopy; EDS, energy dispersive spectroscopy; SQUID, super quantum conducting interference device; PPE, personal protective equipment; GSD, geometric standard deviation

REFERENCES

(1) Jemal, A.; Bray, F.; Center, M.; Ferlay, J.; Ward, E.; Forman, D. Global cancer statistics. *CA—Cancer J. Clin.* **2011**, *61*, 69−90.

(2) American Lung Association. *Lung Cancer Facts and Figures*; 2012. http://www.lung.org/lung-disease/lung-cancer/resources/facts-figures/lung-cancer-fact-sheet.html.

(3) Krapcho, M.; Neyman, N.; Aminou, R.; Howlader, N. *SEER Cancer Statistics Review, 1975−2006*; National Cancer Institute: Bethesda, MD, 2009.

(4) Minchinton, A. I.; Tannock, I. F. Drug penetration in solid tumours. *Nat. Rev. Cancer* **2006**, *6*, 583−592.

(5) Gehr, P.; Bachofen, M.; Weibel, E. R. The normal human lung: ultrastructure and morphometric estimation of diffusion capacity. *Respir. Physiol.* **1978**, *32*, 121−140.

(6) Hershey, A. E.; Kurzman, I.; Forrest, L.; Bohling, C.; Stonerook, M.; Placke, M.; Imondi, A.; Vail, M. Inhalation chemotherapy for macroscopic primary or metastatic lung tumors: proof of principle using dogs with spontaneously occurring tumors as a model. *Clin. Cancer Res.* **1999**, *5*, 2653−9.

(7) Otterson, G. A.; Vilalona-Calero, M.; Sharma, S.; Kris, M.; Imondi, A.; Gerber, M.; White, D.; Ratain, M.; Schiler, J. Sandler. Phase I study of inhaled Doxorubicin for patients with metastatic tumors to the lungs. *Clin. Cancer Res.* **2007**, *13*, 1246−1252.

(8) Otterson, G. A.; Villalona-Calero, M.; Hicks, W.; Pan, X.; Elleron, J.; Gettinger, S.; Murren, J. Phase I/II study of inhaled doxorubicin combined with platinum-based therapy for advanced non-small cell lung cancer. *Clin. Cancer Res.* **2010**, *16*, 2466−2473.

(9) Xie, Y.; Longest, P. W.; Xu, Y. H.; Wang, J. P.; Wiedmann, T. S. In vitro and in vivo lung deposition of coated magnetic aerosol particles. *J. Pharm. Sci.* **2010**, *99*, 4658−4668.

(10) Ally, J.; Amirfazli, A. Chapter 28: Targeting Magnetic Particles for Drug Deliver. In *Handbook of Nanophysics: Nanomedicine and*

Nanorobotics, Sattler, K., Ed.; CRC Press: Boca Raton, **2010**; pp 1−17.
(11) Dames, P.; Gleich, B.; Flemmer, A.; Hajek, K.; Seidl, N.; Wiekhorst, F.; Eberbeck, D.; Bittmann, I.; Bergemann, C.; Weyh, T.; Trahms, L.; Rosenecker, J.; Rudolph, C. Targeted delivery of magnetic aerosol droplets to the lung. *Nat. Nanotechnol.* **2007**, *2*, 495−499.
(12) Rudolph, C.; Gleich, B.; Flemmer, A. W. Magnetic aerosol targeting of nanoparticles to cancer: nanomagnetosols. *Methods Mol. Biol.* **2010**, *624*, 267−280.
(13) McBride, A.; Lamoureux, L.; Price, D.; Muttil, P. Novel Preparation and Characterization of Magnetic Nano-in-Microparticle Dry Powders for Directed Drug Delivery: An Application to Lung Cancer. *Respir. Drug Delivery Conf. 2012* **2012**, *3*, 815−820.
(14) Mikan, A.; Martinez Lanao, J.; Gonzalez Lopez, F.; Dominguez-Gil Hurle, A. High performance liquid chromatography determination of doxorubicin and daunorubicin in plasma using UV detection and column switching. *Biomed. Chromatogr.* **1990**, *4*, 154−156.
(15) Urva, S. R.; Shin, B. S.; Yang, V. C.; Balthasar, J. P. Sensitive high performance liquid chromatographic assay for assessment of doxorubicin pharmacokinetics in mouse plasma and tissues. *J. Chromatogr., B: Anal. Technol. Biomed. Life Sci.* **2009**, *877*, 837−841.
(16) Son, Y.; Mitchell, J.; McConville, J. In Vitro Performance Testing for Pulmonary Drug Delivery. In *Controlled pulmonary drug delivery*, 1st ed.; Smyth, H., Hickey, A.; Springer Publishing Co.: New York, 2011; pp 383−415.
(17) Zak, A.; Feldman, Y.; Lyakhovitskaya, V.; Leitus, G.; Popovitz-Biro, R.; Wachtel, E.; Cohen, H.; Reich, S.; Tenne, R. Alkali metal intercalated fullerene-like MS2 (M= W, Mo) nanoparticles and their properties. *J. Am. Chem. Soc.* **2002**, *124*, 4747−4758.
(18) Tatsumura, T.; Yamamoto, K.; Murakami, A. New chemotherapeutic method for the treatment of tracheal and bronchial cancers–nebulization chemotherapy. *Gan No Rinsho* **1983**, *7*, 765−70.
(19) Louey, M. D.; Van Oort, M.; Hickey, A. J. Aerosol dispersion of respirable particles in narrow size distributions using drug-alone and lactose-blend formulations. *Pharm. Res.* **2004**, *21*, 1207−1213.
(20) Arruebo, M.; Fernández-Pacheco, R.; Ibarra, M. R. Magnetic nanoparticles for drug delivery. *Nano Today* **2007**, *3*, 22−32.
(21) Gupta, A. K.; Gupta, M. Synthesis and surface engineering of iron oxide nanoparticles for biomedical applications. *Biomaterials* **2005**, *26*, 3995−4021.
(22) Gleich, B.; Hellwig, N.; Bridell, H.; Jurgons, R. IEEE Xplore - Design and Evaluation of Magnetic Fields for Nanoparticle Drug Targeting in Cancer. *Nanotechnology* **2007**, *6*, 164−170.
(23) Strable, E.; Bulte, J.; Moskowitz, B. Synthesis and characterization of soluble iron oxide-dendrimer composites. *Chem. Mater.* **2001**, *13*, 2201−2209.
(24) Hasenpusch, G.; Geiger, J.; Wagner, K.; Mykhaylyk, O.; Wiekhorst, F.; Trahms, L.; Heidsieck, A.; Gleich, B.; Rudolph, C. Magnetized Aerosols Comprising Superparamagnetic Iron Oxide Nanoparticles Improve Targeted Drug and Gene Delivery to the Lung. *Pharm. Res.* **2012**, *29*, 1308−18.